Electrochemical modification of active carbon fiber electrode and its application to double-layer capacitor

Toshiyuki Momma [a], Xingjiang Liu [a], Tetsuya Osaka [a], Yousuke Ushio [b], Yoshimitsu Sawada [b]

[a] *Department of Applied Chemistry, School of Science and Engineering, Kagami Memorial Laboratory for Materials Science and Technology, Waseda University, Shinjuku-ku, Tokyo 169, Japan*
[b] *Isuzu Advanced Engineering Center, Ltd., 8 Tsuchidana, Fujisawa, Kanagawa 252 , Japan*

Abstract

Electrochemical oxidation of an active carbon fiber (ACF) electrode showed an enhancement effect of the electrode capacitance. The modification of ACF, however, increased the electrode inner resistance with an increase in the capacitance. Au deposition, the deaeration and the electrochemical reduction (discharge) after the modification showed a decrease in the inner resistance. Thus, the capacitor using the modified ACF electrodes with deaeration, Au deposition and/or discharge treatment showed an enhancement of capacitance with decreasing inner resistance.

1. Introduction

Since an electric double-layer capacitor [1] has a higher power density than that of a small sealed rechargeable battery and also a higher energy density than that of a conventional capacitor, the electric double-layer capacitor has recently come to attract attention for the purpose of a new energy supply [2,3]. As the electrode material for the double-layer capacitor, an active carbon powder [4,5] or fiber [3,6,7] is one of the candidates because of its high specific surface area and high conductivity. The electric double-layer capacity at the electrode surface is usually of the order of about 10–20 $\mu F\,cm^{-2}$ [8], thus a larger specific surface area is demanded to get the larger capacity. The surface area is so important that active carbons having larger surface area are most attractive for the capacitor electrodes. Since the surface conditions of active carbon fiber (ACF) are so sensitive to the capacitance [3,9], some attempts on the modification of the surface condition of the active carbon was extensively examined [9–15]. In this paper, an electrochemical modification of the ACF is proposed to enhance the capacitance of ACF electrodes, and finally the performance of a double-layer capacitor using the treated or modified ACF is discussed.

2. Experimental

The ACF cloth of about 0.024 g having 2000 $m^2\,g^{-1}$ was selected for the electrode. A three-electrode cell was used for the electrochemical measurements of cyclic voltammetry and a.c. impedance spectroscopy. A two-electrode cell was used for the measurements of the capacitor performance, which was constructed with two facing ACF electrodes sandwiching a polypropylene separator. 0.5 M H_2SO_4 was used as the electrolyte solution for all of the electrochemical measurements and the electrochemical treatments. Cyclic voltammograms were obtained at 1.0 mV s^{-1}. The charging and discharging behavior of the conventional capacitor was examined under an application of constant current in the voltage range between 0.2 and 1.0 V.

3. Results and discussion

3.1. Enhancement of capacitance of ACF by electrochemical oxidation and its performance

The ACF electrode showed a typical capacitive behavior in the cyclic voltammogram during potential cycling in the potential window between H_2 and O_2 evolution. A rectangle locus in the voltammograms (see Fig. 1) shows the capacitive currents corresponding to charging or discharging of the electric double layer at the interface between the electrolyte and the ACF surface. In the case of the voltammograms obtained with the scanning potential region extended towards the more positive direction, anodic current appears at over
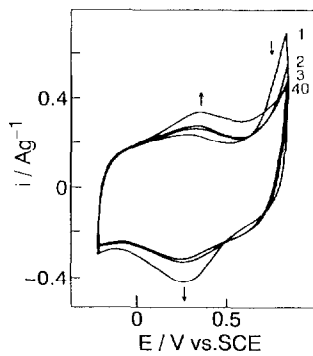
Fig. 1. Cyclic voltammograms for ACF electrode in 0.5 M H_2SO_4 solution at 1 mV s^{-1}. The cycle numbers are illustrated in the figure.

0.6 V versus saturated calomel electrode (SCE), attributed to CO_2 evolution [14]. Fig. 1 shows cyclic voltammograms of an ACF electrode in the potential range between -0.2 and 0.8 V versus SCE in 0.5 M sulfuric acid. In the first cycle the current associated with the CO_2 evolution was observed following the capacitive current. In the subsequent potential scanning, the anodic current of CO_2 evolution decreased and the capacitive current increased. The results indicate that the oxidative treatment of the ACF electrode makes the capacitance higher.

In order to study the oxidation effect on capacitance, a constant anodic potential treatment of ACF electrode was applied as a function of the anodization period as shown in Fig. 2. Under each anodic potential application, the capacitance increases at first with an increase in the oxidizing period, and then decreases with a maximum value. The period showing the maximum capacitance is influenced by the applied potential, and it decreases with an increase in the applied potential. The suitable oxidation condition was determined as the anodic potential supplied at 1.15 V versus SCE for 1 h, and the capacitance of the ACF electrode oxidized under such an optimized condition was about 1.5 times larger than that before oxidation. The oxidation effect of ACF at 1.15 V for 1 h is demonstrated in Fig. 3. The voltammogram of oxidized ACF in Fig. 3 shows an enhanced capacitance with a somewhat retarded current.
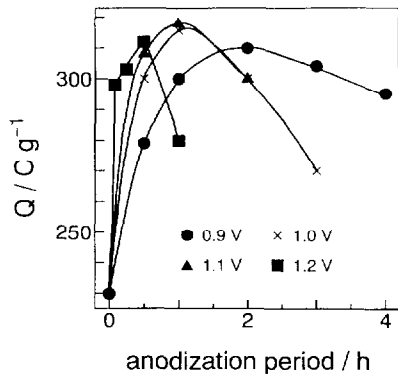

Fig. 2. Relationship between the electrode capacity and anodization period for ACF electrode. The capacity was estimated from the cyclic voltammograms after the oxidation treatment under constant potential. The oxidation potential is shown in the figure (vs. Ag/AgCl).
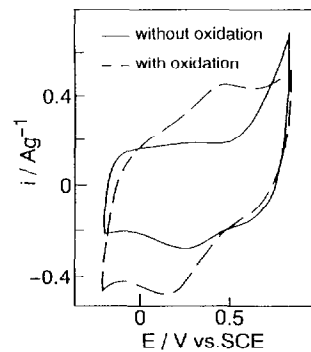

Fig. 3. Cyclic voltammograms at 1 mV s^{-1} for ACF electrodes without (full line) and with (dashed line) oxidation under 1.15 V vs. SCE for 1 h.

The mechanism of this oxidizing capacitance enhancement may be considered to be cleaning of the surface, refining the terminating functional group at the surface or changing of pore size, etc. To probe the mechanism of enhancement, the surface roughness change of the ACF was inspected. In Fig. 4, the morphology change in the ACF electrode by the oxidation is clearly observed. Before the oxidation the surface has many pores with a diameter of 15–35 nm. The oxidative treatment of the ACF makes the surface rougher, and the pores become to be 50–80 nm in diameter. This surface mod-

a) no treatment
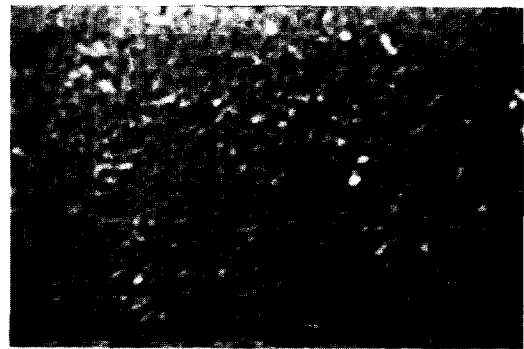
0.5 μm

b) oxidation

0.5 μm

Fig. 4. SEM images for ACF electrodes without and with oxidation under 1.15 V vs. SCE for 1 h.
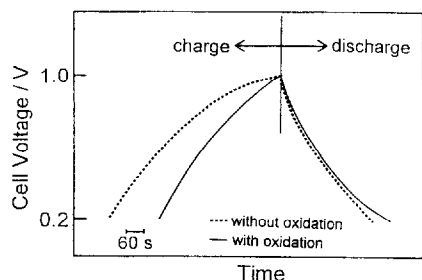
Fig. 5. Charge discharge curves at 0.2 A g^{-1} of capacitors using ACF electrode with and without oxidation.

ification may be due to the chemical attack of generated O_2 or active oxygen on the surface carbon atoms. The surface areas of ACF sample before and after the oxidation were measured using BET adsorption method. The measured values for the ACF before and after the oxidation were 1520 and 1620 m^2 g^{-1}. The increase in surface area coming from the electrochemical oxidation was very small, when compared with the increase in capacitance of the electrode estimated from the voltammograms. The enhancement of the capacitive current is, therefore, considered to be related not only to the increase in surface area but also to the surface condition such as pore size and functional groups of the ACF.

Fig. 5 shows the effect of the electrochemical activation of an ACF electrode on the charge and discharge curves of the capacitors using couples of ACF electrodes. Under constant-current operation with voltage control, the capacitor using the ACF electrodes without oxidation treatment shows longer charging and shorter discharging times than that using oxidized ACF electrodes. The capacity of the capacitors is summarized in Table 1 with a variation of the charge/discharge current density. For both capacitors, the increase in the current density decreases the capacity, as may be due to the solution resistance and the electrode inner resistance. Under loading current density of 0.2 A g^{-1}, the capacitor using oxidized ACF showed an enhanced capacity of about 10%, and was smaller than the value of 315 F g^{-1} measured in the cyclic voltammograms. This may be due to the difference of rest potential of electrodes before the operation of the capacitor. The rest potential of the electrochemically oxidized ACF was about 0.65 V versus SCE, while that of the non-oxidized ACF was about 0.4 V versus SCE. Due to the potential window between − 0.2 and 0.8 V in 0.5 M sulfuric acid for the ACF electrode the positive electrode of the oxidized ACF goes

Table 1
Capacity of the ACF electrode with various treatments. The values were estimated from the charge/discharge tests of the capacitors under various current density

Treatment	Current density (A g^{-1})		
	0.2	4.0	8.0
Without treatment (F g^{-1})	157	144	124
Oxidation (F g^{-1})	170	127	102
Oxidation and discharge (F g^{-1})	204	157	141

easily over the limit of the potential window during the charging process. Thus, the capacitor using the oxidized ACF produces the side reaction of gas evolution during the charging process. In order to avoid such a side reaction the ACF electrodes were discharged under a low constant cathodic current of 0.5 A g^{-1} after the constant potential oxidation. The discharge was terminated when the electrode potential reached 0.15 V versus SCE. The capacitor using the discharged ACF electrodes shows the highest capacity for each loaded current density. From the results, the discharging treatment is clearly effective in enhancing the capacity for the ACF electrode activated with electrochemical oxidation.

3.2. Electrochemical evaluation of oxidized active carbon fiber electrode

In order to examine the inner resistance of the ACF electrode, an a.c. impedance spectroscopy was applied to these various ACF electrodes, since the a.c. impedance analysis distinguishes the resistance and capacitance. The obtained impedance spectra of the ACF electrode are shown in Fig. 6. In the high-frequency region a locus shows two semi-circles and in the low-frequency region the plots align vertically. From the impedance profiles, in the high-frequency region, it is clear that the oxidation and discharge treatment makes the electrode resistance high.

The vertical alignment of impedance plots in the low-frequency region suggests the capacitive behavior of the electrode. The a.c. impedance response for the capacitor is as follows:

$$Z_{imag} = C^{-1}\omega^{-1} \tag{1}$$

where ω, Z_{imag}, and C are the angular velocity, the imaginary component of the impedance, and the capacitance of the electrode, respectively. In Fig. 7, the Z_{imag} profiles of the non-treated ACF and the oxidized, discharged ACF electrodes are shown as a function of ω^{-1}. From the slope of these relationships the electrode capacitance is calculated, and the results were 156 and 220 F g^{-1} for ACF without treatment and ACF with oxidation and discharge, respectively.

In Fig. 6, the resistance component can be analyzed in the high frequency region. Two components of a semi-circle in the high-frequency responses exist in both spectra. Therefore, we have to consider two components for the equivalent circuit for the ACF electrode, namely, the circuit shown in Fig. 8. The estimated parameters were summarized in Table 2. With consideration of the values of resistance and capacitance, the physical explanation for each component will become clear. Only the component of R_2 shows a drastic change by the oxidation and discharge treatment, while the other parameters, such as R_1, C_1 and C_2 show small changes. The values of C_1 and C_2 are of the order of 1 and 100 mF g^{-1}, while the electrode capacitance is as large as 156 or 220 F g^{-1}. Thus, we can conclude the physical meanings of each component
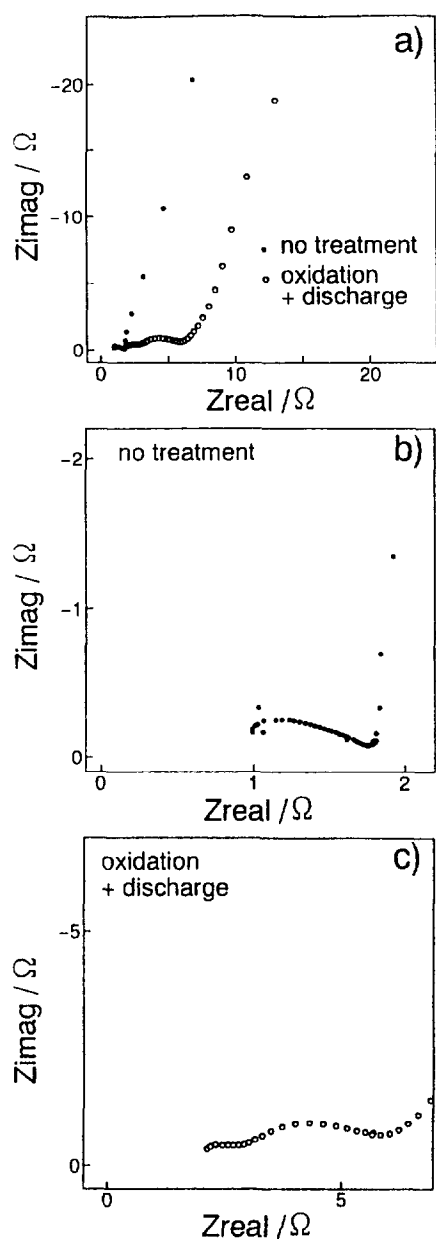
Fig. 6. (a). Cole–Cole plots for ACF electrodes without and with oxidation and discharge treatments. (b) and (c) are the magnified plots of each plot.
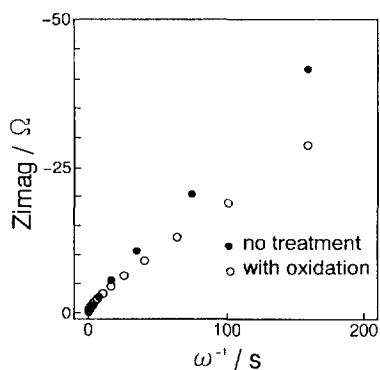

Fig. 7. Relationship between the imaginary component of the ACF impedance in low frequency region and the angular velocity.
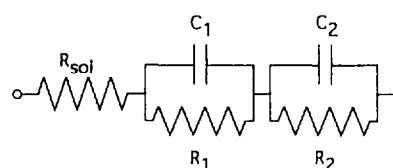

Fig. 8. The equivalent circuit for the impedance spectra of ACF electrode.

Table 2
Components of the equivalent circuit fitted for the impedance spectra

Treatment	First circle		Second circle	
	R_1 Ω (mΩ g)	C_1 μF (mF g^{-1})	R_2 Ω (mΩ g)	C_2 mF (F g^{-1})
Without treatment	0.6 (14)	80 (3.3)	0.2 (4.8)	5.0 (0.21)
Oxidation and discharge	0.9 (22)	40 (1.7)	3.0 (72)	2.5 (0.10)

as follows. The component composed of C_1 and R_1 is due to the impedance between the ACF and the backing plate for the electrical connection, because the capacitance of the backing plate is equal to the C_1 value. The R_1 is therefore due to the resistance between the backing plate and the ACF. The capacitance value of C_2 locates between the C_1 value and the whole electrode capacitance, and the R_2 value becomes 10 times larger by the oxidation and discharge treatment. Since the electrochemical oxidation causes the surface morphology of ACF to roughen to make micropores as is seen in Fig. 4, the resistance between the carbon fibers in ACF may increase due to lessening the contacting area of each fiber. Thus, the components of R_1 and C_1 are the inner resistance and capacitance of ACF electrode.

3.3. Decrease of inner resistance and capacitor performance

From the impedance analysis of ACF electrodes, it is clear that the treatment of ACF using oxidation and discharge is effective for the enhancement of the electrode capacitance, while it makes the electrode inner resistance high. In order to decrease the inner resistance of the oxidized and discharged ACF electrode, deaeration and gold evaporation were attempted.

After application of the electrochemical oxidation and discharge, the ACF electrode may contain gas bubbles within the electrode. The deaeration of the ACF in the electrolyte solution under vacuum conditions drives such small bubbles out from the electrode. The gold vapor deposition makes the electrical contact between the carbon fibers very good. In Fig. 9, the impedance spectra are shown for the ACF electrodes with deaeration or gold vapor deposition after the oxidation and discharge treatment. The whole electrode capacitance of ACF with gold deposition was 223 F g^{-1} and the sample with gold deposition and deaeration was 226 F g^{-1}. There does not appear to be a significant change in the capacitance value, while both treatments of deaeration
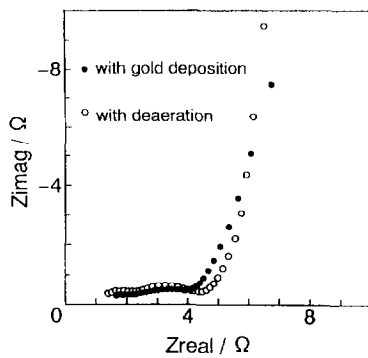
Fig. 9. Cole–Cole plots for the ACF electrodes with pretreatments of gold deposition or deaeration.

Table 3
Capacity of the oxidized discharged ACF electrode with deaerated and gold deposited treatment. The values were estimated from the charge/discharge tests of the capacitor under various current densities

Current density (A g^{-1})	0.2	4.0	8.0
Capacitance (F g^{-1})	220	178	162

and gold deposition cause a decrease in the inner resistance of the ACF. From the results, the ACF electrode with the treatment of both deaeration and gold deposition after oxidation and discharge is thought to give the most enhanced capacitance with the lowest inner resistance.

The capacity of the capacitor using such optimized ACF electrodes is shown in Table 3 with a variation of loading current density. The capacitance measured at 0.2 A g^{-1} is almost equal to the value estimated from the impedance analysis, and even under loading of 4 or 8 A g^{-1} the capacitance does not show significant decreases.

4. Conclusions

The application of electrochemical oxidation on the ACF electrode showed an increase in the double-layer capacitance. The discharge treatment after the oxidation was effective for application of the ACF to the capacitor electrodes. The oxidized ACF had an increased inner resistance, while the resistance was decreased by deaeration and Au deposition on the back side. The capacitor using resulting ACF electrodes was revealed to give an enhanced performance.

References

[1] H.I. Becker, Low voltage electrolytic capacitor, US Patent No. 2 800 616 (1957).
[2] S. Sekido, T. Muranaka, Y. Yoshino and H. Mori, Nat. Tech. Rep., 26 (1980) 220.
[3] A. Nishino, A. Yoshida, I. Tanahashi, I. Tajima, M. Yamashita, T. Muranaka and H. Yoshida, Nat. Tech. Rep., 31 (1985) 318.
[4] T. Kanbara, K. Nishimura and T. Yamamoto, J. Power Sources, 32 (1990) 165.
[5] I. Tanahashi, A. Yoshida and A. Nishino, Bull. Chem. Soc. Jpn., 63 (1990) 2755.
[6] I. Tanahashi, A. Yoshida and A. Nishino, Bull. Chem. Soc. Jpn., 63 (1990) 3611.
[7] I. Tanahashi, A. Yoshida and A. Nishino, J. Electrochem. Soc., 137 (1990) 3052.
[8] B. Kastening, W. Schiel and M. Henschel, J. Electroanal. Chem., 191 (1985) 311.
[9] A. Yoshida, I. Tanahashi and A. Nishino, Carbon, 28 (1990) 611.
[10] I. Tanahashi, A. Yoshida and A. Nishino, J. Appl. Electrochem., 21 (1991) 28.
[11] A. Proctor and P.M.A. Sherwood, Carbon, 21 (1983) 53.
[12] R. Fu, H. Zeng and Y. Lu, Carbon, 32 (1994) 593.
[13] A.D. Jannakoudakis, P.D. Jannakoudakis and E. Theodoridou, J. Appl. Electrochem., 20 (1990) 619.
[14] K. Kinoshita and J.A.S. Bett, Carbon, 11 (1973) 403.
[15] K. Kinoshita, in K. Kinoshita (ed.), Carbon, Electrochemical and Physicochemical Properties, Wiley, New York, 1988, p.293.